

Neuro-Oncology

Neuro-Oncology 18(7), 962–973, 2016

doi:10.1093/neuonc/nov321

Advance Access date 28 January 2016

Core pathway mutations induce de-differentiation of murine astrocytes into glioblastoma stem cells that are sensitive to radiation but resistant to temozolomide

Ralf S. Schmid, Jeremy M. Simon, Mark Vitucci, Robert S. McNeill, Ryan E. Bash, Andrea M. Werneke, Lauren Huey, Kristen K. White, Matthew G. Ewend, Jing Wu, and C. Ryan Miller

Lineberger Comprehensive Cancer Center, University of North Carolina School of Medicine, Chapel Hill, North Carolina (R.S.S., L.H., M.G.E., J.W., C.R.M.); Division of Neuropathology, Department of Pathology & Laboratory Medicine, University of North Carolina School of Medicine, Chapel Hill, North Carolina (M.V., R.S.M., R.E.B., A.M.W., K.K.W., C.R.M.); Carolina Institute for Developmental Disabilities and Department of Genetics, University of North Carolina School of Medicine, Chapel Hill, North Carolina (J.M.S.); Department of Neurosurgery, University of North Carolina School of Medicine, Chapel Hill, North Carolina (M.G.E., J.W.); Department of Neurology and Neurosciences Center, University of North Carolina School of Medicine, Chapel Hill, North Carolina (C.R.M.)

Corresponding Author: C. Ryan Miller, MD, PhD, University of North Carolina School of Medicine, 6109B Neurosciences Research Building, Campus Box 7250, Chapel Hill, NC 27599-7250 (rmiller@med.unc.edu).

Background. Glioma stem cells (GSCs) from human glioblastomas (GBMs) are resistant to radiation and chemotherapy and may drive recurrence. Treatment efficacy may depend on GSCs, expression of DNA repair enzymes such as methylguanine methyltransferase (MGMT), or transcriptome subtype.

Methods. To model genetic alterations in human GBM core signaling pathways, we induced Rb knockout, Kras activation, and Pten deletion mutations in cortical murine astrocytes. Neurosphere culture, differentiation, and orthotopic transplantation assays were used to assess whether these mutations induced de-differentiation into GSCs. Genome-wide chromatin landscape alterations and expression profiles were examined by formaldehyde-assisted isolation of regulatory elements (FAIRE) seq and RNA-seq. Radiation and temozolomide efficacy were examined in vitro and in an allograft model in vivo. Effects of radiation on transcriptome subtype were examined by microarray expression profiling.

Results. Cultured triple mutant astrocytes gained unlimited self-renewal and multilineage differentiation capacity. These cells harbored significantly altered chromatin landscapes that were associated with downregulation of astrocyte- and upregulation of stem cell-associated genes, particularly the *Hoxa* locus of embryonic transcription factors. Triple-mutant astrocytes formed serially transplantable glioblastoma allografts that were sensitive to radiation but expressed MGMT and were resistant to temozolomide. Radiation induced a shift in transcriptome subtype of GBM allografts from proneural to mesenchymal.

Conclusion. A defined set of core signaling pathway mutations induces de-differentiation of cortical murine astrocytes into GSCs with altered chromatin landscapes and transcriptomes. This non-germline genetically engineered mouse model mimics human proneural GBM on histopathological, molecular, and treatment response levels. It may be useful for dissecting the mechanisms of treatment resistance and developing more effective therapies.

Keywords: Astrocytes, glioblastoma, glioma stem cells, radiation, temozolomide.

Brain tumors are among the most devastating of all human cancers. Survival for glioblastoma (GBM), the most common and biologically aggressive brain tumor, averages 12–15 months.¹ Standard therapy for newly diagnosed GBM patients consists of surgery followed by radiation therapy (XRT) with concurrent and adjuvant temozolomide (TMZ). This regimen produces a modest, 3-month improvement in survival

compared with XRT alone but invariably fails to prevent tumor recurrence.²

Factors that may drive GBM recurrence include the presence of cancer stem cells (CSCs), inherent resistance to DNA-damaging therapies, and transcriptome subtype. The CSC hypothesis posits that tumor cells with stem cell-like properties (referred to generically as CSCs or specifically as brain tumor

Received 8 May 2015; accepted 14 December 2015

© The Author(s) 2016. Published by Oxford University Press on behalf of the Society for Neuro-Oncology. All rights reserved.

For permissions, please e-mail: journals.permissions@oup.com.

or glioma stem cells [GSCs] are responsible for tumor maintenance.^{3–5} GSCs share properties with neural stem cells (NSCs), including their capacity to undergo unlimited self-renewal and to differentiate into multiple neural cell lineages, and can generate the full cellular complexity of a tumor. GSCs may be inherently resistant to XRT and many chemotherapeutic agents and thus may be responsible for tumor recurrence.^{6,7} The DNA repair protein MGMT, an enzyme dedicated to repair of alkyl-nucleotide adducts, is an important modulator of chemoresistance to alkylating agents used in GBM treatment including TMZ and the nitrosoureas carmustine (BCNU) and lomustine (CCNU).^{8,9} Methylation-based silencing of the *MGMT* promoter has been proposed as a predictive biomarker for identifying TMZ responders.^{8–10} Genomic analyses of GBM have identified frequently mutated genes in 3 core signaling pathways: the G1/S cell cycle checkpoint (Rb), receptor tyrosine kinase (RTK)/mitogen activated protein kinase (MAPK)/phosphoinositide 3 kinase (PI3K), and TP53 pathways.¹¹ Transcriptome profiling has been used to classify GBM into 4 molecular subtypes (proneural, neural, classical, and mesenchymal) with inherent differences in response to DNA-damaging therapies such as XRT and TMZ.^{10–14}

Genetically engineered mouse (GEM) models faithfully recapitulate the molecular genetics and biology of human gliomas. These models have emerged as an essential experimental tool for investigating glioma genetics and evaluating novel therapeutics.^{15,16} We previously developed a non-germline GEM (nGEM) model of GBM using cortical astrocytes harvested from mice with conditional oncogenic alleles in core signaling pathway genes. Mutations that ablate the G1/S checkpoint and activate MAPK and PI3K signaling—specifically inhibition of the Rb family of pocket proteins via an N-terminal, 121 amino acid truncation mutant of SV40 large T antigen (T₁₂₁, T) expressed from the human glial fibrillary acidic protein (GFAP) promoter, a constitutively active *Kras* mutant (*Kras*^{G12D}, R), and deletion of the negative PI3K regulator *Pten* (P), respectively—transform cultured TRP astrocytes, modulate their metabolism, and induce a primitive, proneural GBM-like gene expression state.^{17–19} Moreover, orthotopic injection of TRP astrocytes into the brains of syngeneic, immunocompetent mice produces rapidly fatal GBM.¹⁷

Here we demonstrate that TRP mutations induce astrocyte de-differentiation and that these cells have altered chromatin landscapes and gene expression profiles. TRP astrocytes gain the functional properties of GSCs *in vitro* and develop into serially transplantable GBM when as few as 100 cells are orthotopically allografted *in vivo*. We then examine the role of MGMT in TMZ sensitivity and transcriptome response to XRT. TRP astrocytes and allografts express MGMT and are resistant to TMZ. XRT induces a transient inhibition of tumor growth and a significant increase in survival. Transcriptome analyses show that TRP allografts are enriched for human proneural GBM signatures and that XRT induces a mesenchymal shift in transcriptome phenotype, similar to its effects in human GBM.^{12,13}

Materials and Methods

Genetically Engineered Mice

Crossing heterozygous conditional *TgGZT*₁₂₁ (T), heterozygous *Kras*^{G12D} conditional knock-in (R), and/or homozygous conditional

Pten knock-out (P) mice generated compound T, TR, and TRP mice.^{17,20,21} PCR genotyping was performed as previously described.¹⁷ The University of North Carolina Institutional Animal Care and Use Committee approved all animal studies.

Orthotopic Allografts and Xenografts

Mutant astrocytes were allografted into syngeneic C57Bl/6 hosts as previously described.¹⁷ Xenograft experiments used athymic nude mice (Charles River), which were orthotopically injected with U87FL cells.²²

Microarray and Sequencing Data

Original microarray (GSE59116) and sequencing (GSE75592) data have been deposited into Gene Expression Omnibus.

Statistics

Data were analyzed with GraphPad Prism 5 or Stata 12 (Stata-Corp). All comparisons were considered significant at $\alpha = 0.05$.

Results

Core Glioblastoma Pathway Mutations Induce Astrocyte De-differentiation Into Glioma Stem Cells

We have shown that RP mutations activate MAPK and PI3K signaling in T₁₂₁-expressing astrocytes with a defective G1/S checkpoint and cooperate to potentiate proliferation, migration, and invasion *in vitro*. Moreover, triple-mutant TRP astrocytes are tumorigenic, producing tumors with histology similar to human GBM *in vivo*.^{17,18} However, it remained unclear whether they also induced GSC phenotypes.

GSCs express NSC markers, display unlimited self-renewal, are capable of multilineage differentiation, and are tumorigenic when serially transplanted into mouse brains. We first examined whether TRP astrocytes gained expression of NSC/GSC markers (Supplementary material, Fig. S1, Supplementary material, Table S1). NSCs harvested from the subventricular zone of wild-type mice expressed CD133, Sox2, and Nestin, and a subset expressed GFAP (Supplementary material, Fig. S1A). Wild-type astrocytes expressed GFAP but lacked NSC/GSC markers (Supplementary material, Fig. S1B). TRP astrocytes maintained GFAP, and Cre recombination induced T₁₂₁, CD133, Sox2, and Nestin expression (Supplementary material, Fig. S1C). These results indicate that TRP mutations induce NSC/GSC marker expression in cultured astrocytes.

Self-renewal capacity was examined by growing TRP astrocytes as nonadherent neurospheres in growth factor-defined media. Neurospheres could be serially propagated for at least 6 passages, and frequency was comparable to wild-type NSCs (Fig. 1A). Wild-type and un-recombined TRP astrocytes failed to form neurospheres (data not shown). These results suggest that TRP astrocytes undergo unlimited self-renewal similar to wild-type NSCs.

We next examined whether TRP neurospheres were multipotent. Reintroduction of serum induced differentiation into GFAP⁺ astrocytes (Fig. 1B), NG2⁺ oligodendrocyte progenitor cells (OPCs), and Tuj1⁺ neurons (Fig. 1C). Similar results were obtained with wild-type NSC neurospheres (data not shown).

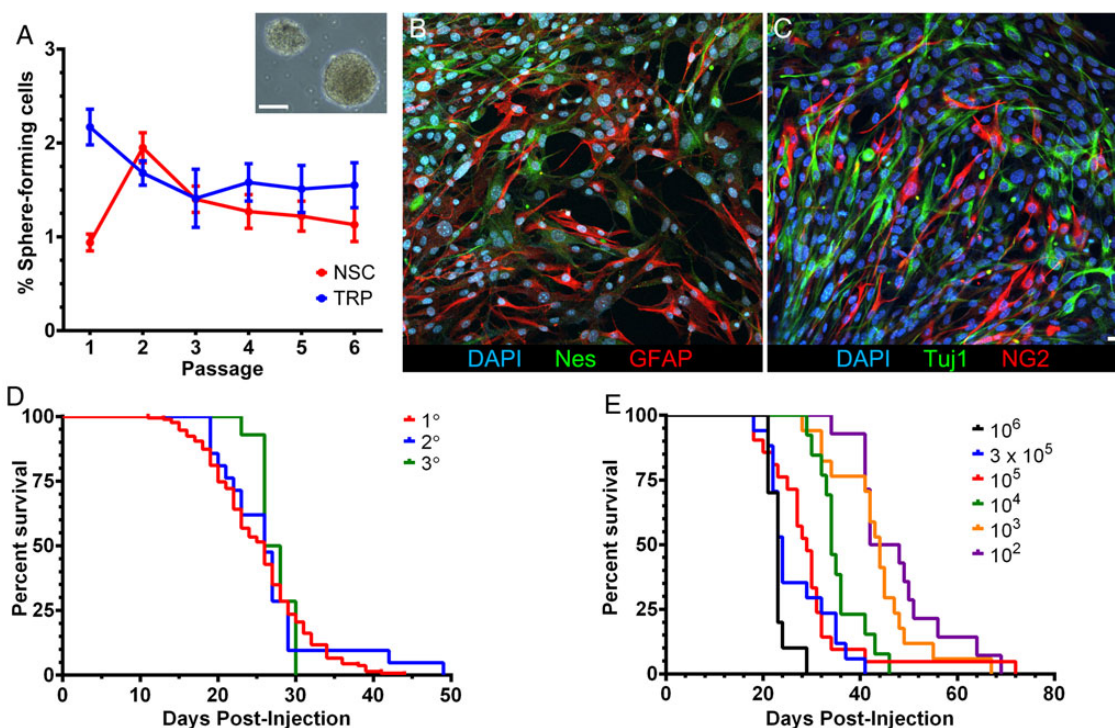


Fig. 1. TRP astrocytes acquire glioma stem cell features in vitro and in vivo. Neurosphere self-renewal of TRP astrocytes was indistinguishable from wild-type neural stem cells ($P \geq .1$). Scale bar = 50 μm (A). Serum-induced differentiation of nestin⁺ TRP neurospheres into glial fibrillary acidic protein-positive astrocytes (B), NG2⁺ oligodendroglia, and Tuj1⁺ neurons (C). Scale bar = 10 μm . Primary TRP allografts were serially transplantable into secondary and tertiary host brains. Median survival (26–27 d) was indistinguishable ($P = .8$), and all mice developed glioblastoma (D). A cell dose-dependent (10^2 – 10^6) increase in median survival (23–45 d) was evident ($P < .0001$, E).

These results demonstrated that TRP mutations induce astrocyte de-differentiation and that these cells acquire NSC properties in vitro.

We also examined T and TR astrocytes to determine whether RP mutations were required to induce de-differentiation. Since T, TR, and TRP astrocytes could be serially propagated as neurospheres in defined media, we estimated the frequency of stem cells in each using an extreme limiting-dilution assay (Fig. 2A). Wild-type astrocytes failed to form neurospheres in this assay as well (data not shown). TRP astrocytes contained significantly more neurosphere-forming stem cells than T and TR astrocytes but less than NSCs (Supplementary material, Fig. S2A). However, serum induced multilineage differentiation in all 3 genotypes (Fig. 2B and Supplementary material, Fig. S2B–D). Thus, while T and TR astrocytes acquired NSC properties, their stem cell frequency was significantly less than TRP astrocytes. These results suggested that ablation of the G1/S checkpoint by T₁₂₁ alone is sufficient to form multipotent neurospheres, but all 3 mutations are required to significantly increase stem cell frequency.

In addition to NSC properties, GSCs are also capable of producing tumors upon serial transplantation. Indeed, TRP astrocytes produced astrocytomas in 100% of injected mice, and survival was highly reproducible (Supplementary material, Fig. S3A). GBM developed in all secondary and tertiary hosts, and survival was identical (Fig. 1D). Furthermore, serial dilutions produced a dose-dependent increase in survival, but all mice

succumbed to GBM from as few as 100 transplanted cells (Fig. 1E and Supplementary material, Fig. S3B). These findings are consistent with the 1%–2% neurosphere-forming efficiency in vitro (Fig. 1A). Taken together, these results demonstrate that TRP astrocytes behave as GSCs in vivo.

Because the vast majority of TRP-allografted mice developed GBM when aged to neurological morbidity, we examined whether these tumors progressed histologically. Mice were systematically euthanized at 5-day intervals, and their brains were examined (Supplementary material, Figs. S3C and S4). At 5 days, 60% of mice had developed small, mitotically active anaplastic astrocytomas (WHO grade III) that diffusely invaded brain parenchyma (Supplementary material, Fig. S4A–C). By 20 days, all mice had developed progressively larger, mitotically active GBM (WHO grade IV) with microvascular proliferation and necrosis (Supplementary material, Fig. S4J–L). Only 30% of mice injected with T astrocytes developed small low-grade astrocytomas (<1 mm²) that required 12 months to grow (Fig. 2C–E).¹⁷ TR astrocytes produced tumors less frequently (16%), but these were larger and higher grade and required significantly less time to develop. In contrast, mice injected with TRP astrocytes developed large, high-grade tumors that required markedly less time to develop. These results suggest that while T and TR astrocytes acquire NSC properties in vitro, simultaneous ablation of the G1/S checkpoint and activation of both MAPK and PI3K signaling are required to convert astrocytes into highly potent, tumorigenic GSCs in vivo.

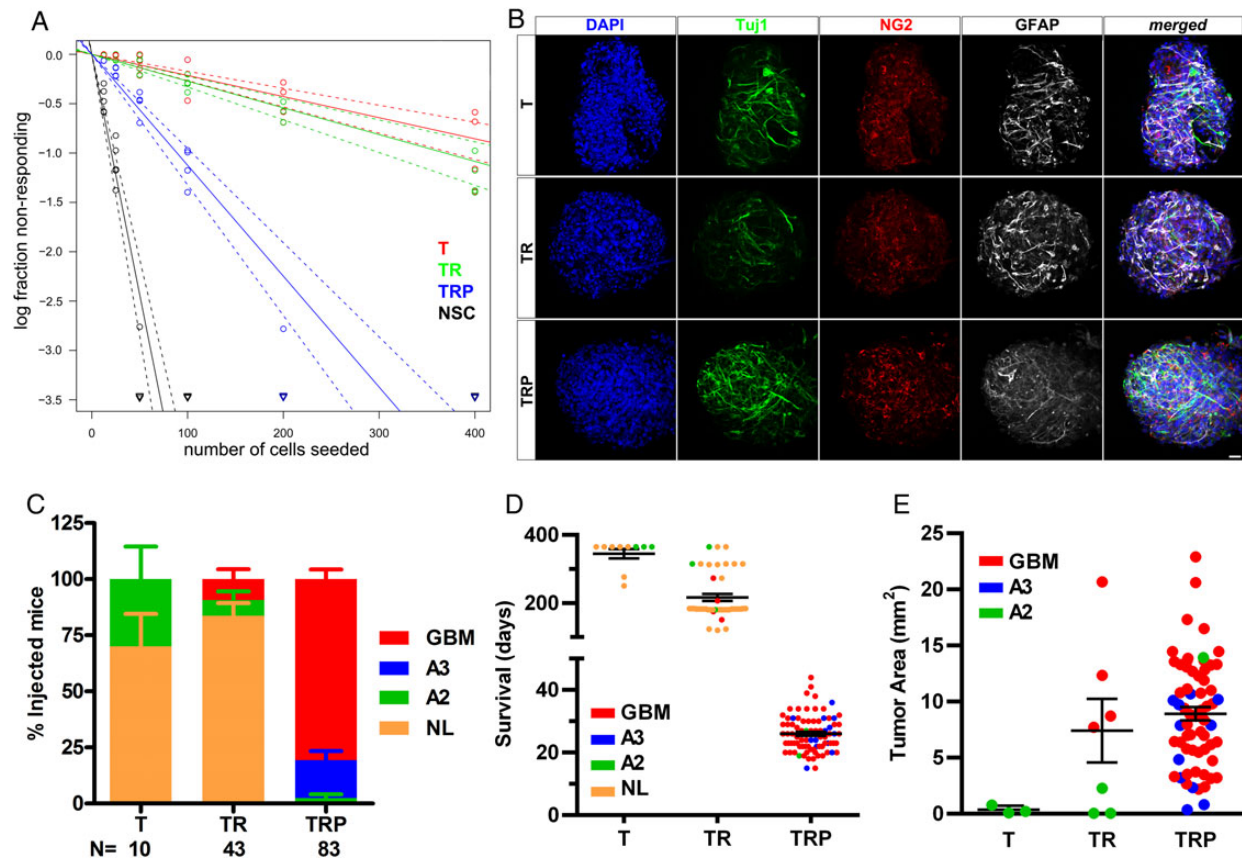


Fig. 2. G1/S ablation and activating MAPK and PI3K mutations are required to induce efficient astrocyte de-differentiation and tumorigenesis. TRP astrocytes contained significantly more neurosphere-forming stem cells than T and TR astrocytes but less than neural stem cells (1 in 21) (Supplementary material, Fig. S2A) (A). Serum-induced differentiation of T, TR, and TRP neurospheres into glial fibrillary acidic protein-positive astrocytes, NG2⁺ oligodendroglia, and Tuj1⁺ neurons (B). TRP astrocytes developed into astrocytomas in all mice, but T and TR astrocytes failed to develop tumors in >70% ($P < .0001$, C). Mice injected with 10^5 TRP astrocytes required significantly less time (26.0 ± 0.6 d) to develop tumors than T (345 ± 13.6 d) and TR (216 ± 10.6 d) astrocytes ($P < .0001$, D). T astrocyte tumors were significantly smaller (mean 0.4 ± 0.2 mm²) than TR (mean 7.4 ± 2.8 mm²) or TRP (mean 8.9 ± 0.6 mm²) astrocyte tumors ($P = .016$, E). N, number of mice examined; NL, normal; A2, diffuse astrocytoma (WHO grade II); A3, anaplastic astrocytoma (WHO grade III); GBM, glioblastoma (WHO grade IV). Scale bars = 10 μ m.

Core Glioblastoma Pathway Mutations Induce Global Changes in the Astrocyte Chromatin Landscape

Differentiation and cellular identity are epigenetically regulated. Genome-wide profiling methods, such as formaldehyde-assisted isolation of regulatory elements (FAIRE)-seq, have been developed to globally assess chromatin landscapes and the role of open chromatin regions (regulatory elements) in cellular identity.^{23,24} We therefore used FAIRE-seq to define open chromatin regions in cultured wild-type astrocytes and assess how mutations altered their chromatin landscape. Hierarchical clustering (Fig. 3A) and principal components analysis (Fig. 3B) on highly variable regions (Supplementary material, Table S2) showed that the chromatin landscapes of all 4 genotypes were distinct. Regions clustered into 4 classes, each enriched in particular astrocyte genotypes. TRP astrocyte-enriched regions contained genes shown to promote GBM tumorigenesis including *Vav3* (Fig. 3C) and *Hdac9* (Fig. 3D).^{25,26} Regions enriched in wild-type astrocytes contained genes shown to decrease GSC tumorigenesis including *Snai1* (Fig. 3E).²⁷

Next, we used bioinformatic tools to identify enriched ontologies of nearby genes and motifs corresponding to known transcription factors within regions of open chromatin. TRP astrocyte-enriched regions demonstrated linkages with developmental and stem cell processes (Supplementary material, Table S3). Although sites within all 4 classes harbored motifs for important stem cell transcription factor families, only the TRP-enriched cluster contained multiple families including Nanog and Sox (Fig. 3F).

RNA-seq analysis of TRP and wild-type astrocytes revealed significant alterations in the mutated astrocyte transcriptome (2257 of 20 733 genes, 10.9%, Fig. 4A, Supplementary material, Table S4). TRP mutations induced downregulation of astrocyte signature genes (Fig. 4B, Supplementary material, Table S5) and upregulation of stem cell-related genes.^{28–31} Decreased expression of the astrocyte-specific genes *Aqp4* (Fig. 4C), *Aldh1l1*, and *Fgfr3* (data not shown) correlated with decreased promoter chromatin accessibility (Supplementary material, Table S6). In contrast, promoters within the *Hoxa* locus on chromosome 6 showed increased accessibility, and

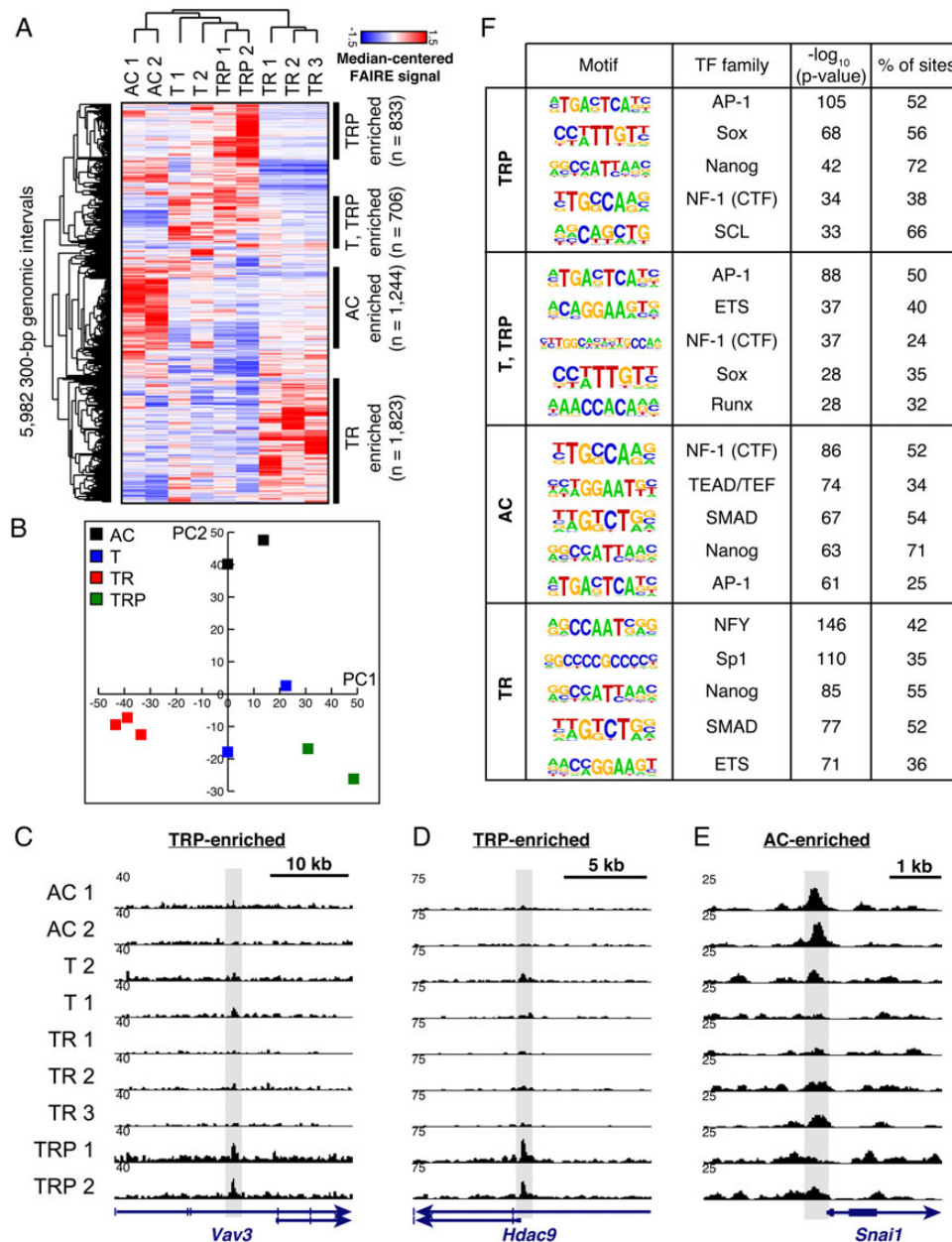


Fig. 3. TRP mutations induce genome-wide alterations in the chromatin landscape of astrocytes. Highly variable intervals (300 bp) of open chromatin were analyzed by hierarchical clustering. Regions of increased chromatin accessibility were enriched in TRP, T and TRP, TR, or wild-type astrocytes (AC) (A). Principal component analysis confirmed that chromatin landscapes of these cells were distinct (B). Representative genes from TRP-enriched (CD) and AC-enriched (E) regions are shown. Target motifs specific to particular transcription factor (TF) families were enriched in each class, but only the TRP class harbored motifs from multiple families of stem-cell TF (F).

Hoxa1-7 and *Hoxa9* expression was increased >4-fold in TRP astrocytes (Fig. 4D, Supplementary material, Tables S4 and S6). The Hox family of stem-cell transcription factors are important for embryonic development, and their dysregulated expression has been found in various cancers including GBM.^{32,33} To determine whether these gene expression changes were significant among all significantly altered pathways, we performed and aggregated an analysis of gene ontologies (Supplementary material, Table S7). We found that TRP astrocytes exhibited

upregulation of genes involved with cell growth and embryonic development (Fig. 4E) and a concomitant loss of neural and cell adhesion-related processes (Fig. 4F).

TRP Astrocytes Are Sensitive to Radiation Therapy but Are Resistant to Temozolomide due to MGMT

Fractionated XRT and TMZ are standard therapy for GBM.² GSCs are frequently resistant to these therapies.^{6,7} We therefore

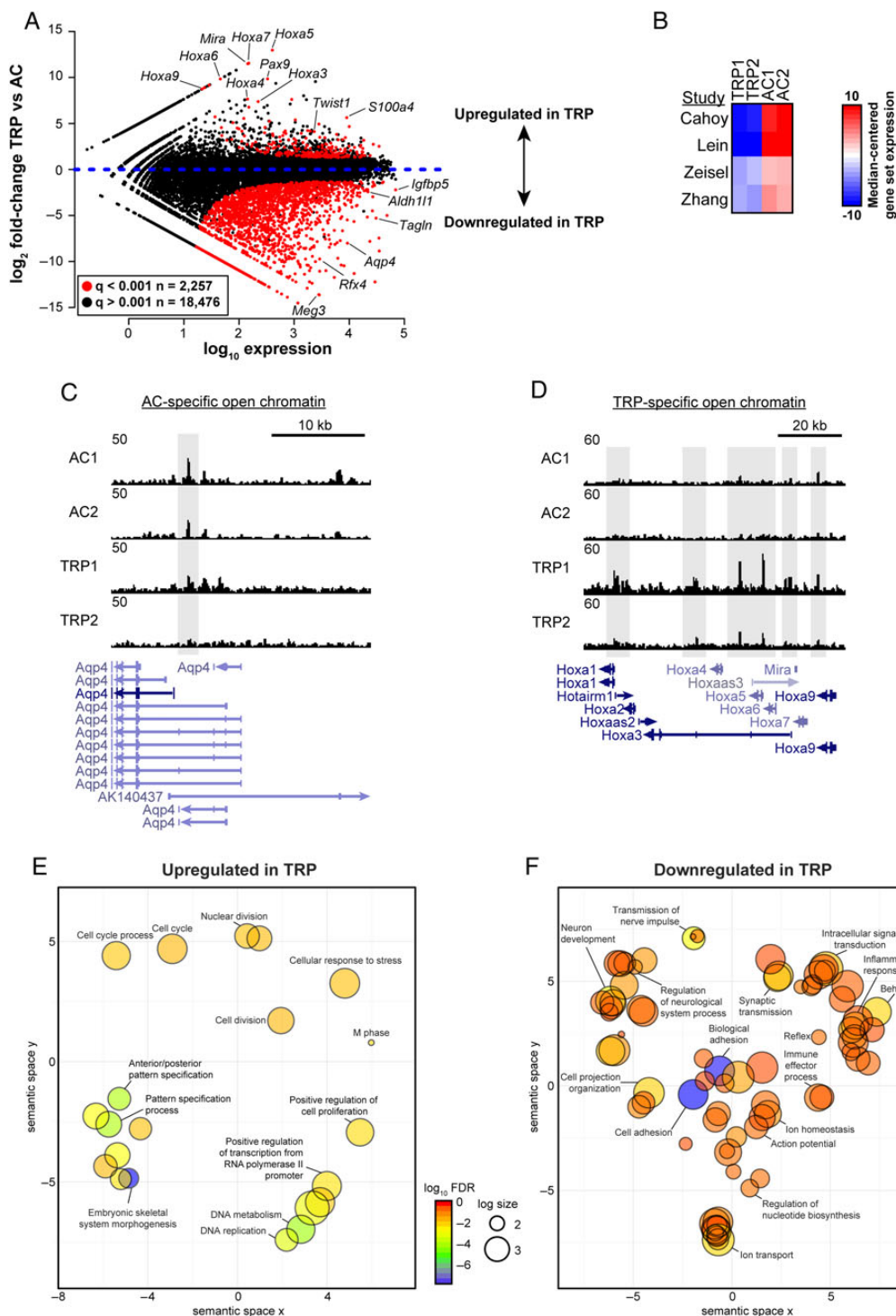


Fig. 4. TRP mutations induce downregulation of astrocyte markers and upregulation of stemness genes. Differential expression analysis showed that TRP mutations induced significant transcriptome alterations (10.9%, $q < 0.001$) relative to wild-type astrocytes (A), including downregulation of published astrocyte gene signatures (B, $FDR < 0.01$). Decreased expression of the astrocyte-specific gene *Aqp4* (C) and increased expression of the *Hoxa* locus of stem cell transcription factors (D) anti-correlated with chromatin accessibility alterations within 70KB of their transcriptional start sites. An aggregated gene ontology analysis showed upregulation of cell growth and embryonic development (E) and downregulation of neural and cell adhesion-related processes (F). FDR values are colored; diameter indicates term frequency.

examined whether TRP astrocytes were sensitive to XRT and TMZ. To provide a frame of reference, human U87 cells were also examined because they have been widely studied, and their sensitivity to cytotoxic therapies has been defined.^{22,34,35} XRT sensitivity of TRP astrocytes was similar to U87 (Fig. 5A) and other human GBM cell lines.^{22,36,37} TMZ inhibited U87 growth at 31-fold lower concentrations than TRP astrocytes (Fig. 5B) and induced G2/M arrest only in U87 cells (Supplementary material, Fig. S5). Because TMZ IC_{50} was >10-fold higher than maximal plasma levels of orally administered TMZ (50 μ M), we concluded that TRP astrocytes are highly resistant to TMZ in vitro.³⁸ To examine whether TRP mutations induced acquired resistance, TMZ sensitivity of wild-type, T, and TR astrocytes as well as wild-type NSCs was also examined. All were highly resistant, suggesting that resistance was not acquired during the process of transformation (Supplementary material, Fig. S6).

Expression of the DNA repair enzyme MGMT is an established TMZ resistance mechanism.⁸ MGMT expression was therefore examined in TRP astrocytes, wild-type NSCs, and astrocytes by immunoblot. All 3 expressed similar levels of MGMT (Supplementary material, Fig. S7A and B), but MGMT was 3.5-fold higher in TRP astrocytes than U87 cells (Fig. 5C). These results suggest that TRP astrocytes, as well as wild-type NSCs, are resistant to TMZ due to MGMT. To confirm this hypothesis, O⁶-benzylguanine (O⁶-BG) was used to inhibit MGMT pharmacologically. O⁶-BG produced a dose-dependent increase in TMZ sensitivity, and IC_{50}

decreased ~10-fold in the presence of 75 μ M O⁶-BG (Fig. 5D and E). O⁶-BG did not significantly alter U87 response (Supplementary material, Fig. S7C and D), a finding consistent with other established human GBM cell lines.³⁹ TRP astrocytes and U87 cells responded similarly to 2 mechanistically related DNA alkylating agents, the nitrosoureas BCNU and CCNU (Supplementary material, Fig. S8A and B), and neither was sensitive at plasma concentrations (~10 μ M) achieved in patients.^{35,36} MGMT inhibition with O⁶-BG did not alter sensitivity to these drugs (Supplementary material, Fig. S8C and D). To determine whether TRP astrocyte resistance was specific for alkylating agents or applied more globally to other cytotoxic agents, their sensitivity to SN-38, an active metabolite of the mechanistically distinct topoisomerase I inhibitor irinotecan, was examined. Both TRP astrocytes and U87 cells were sensitive to SN-38 (Supplementary material, Fig. S8E) at concentrations well below those achieved clinically (~250 nM).⁴⁰ These results suggest that TRP astrocytes are inherently resistant to DNA alkylating agents, but not other cytotoxic drugs, and that MGMT contributes to their TMZ resistance.

TRP Allografts Are Sensitive to Radiation Therapy but Resistant to Temozolomide

Efficacy of TMZ, XRT, or their combination was examined in mice bearing established orthotopic TRP allografts. TMZ dose and

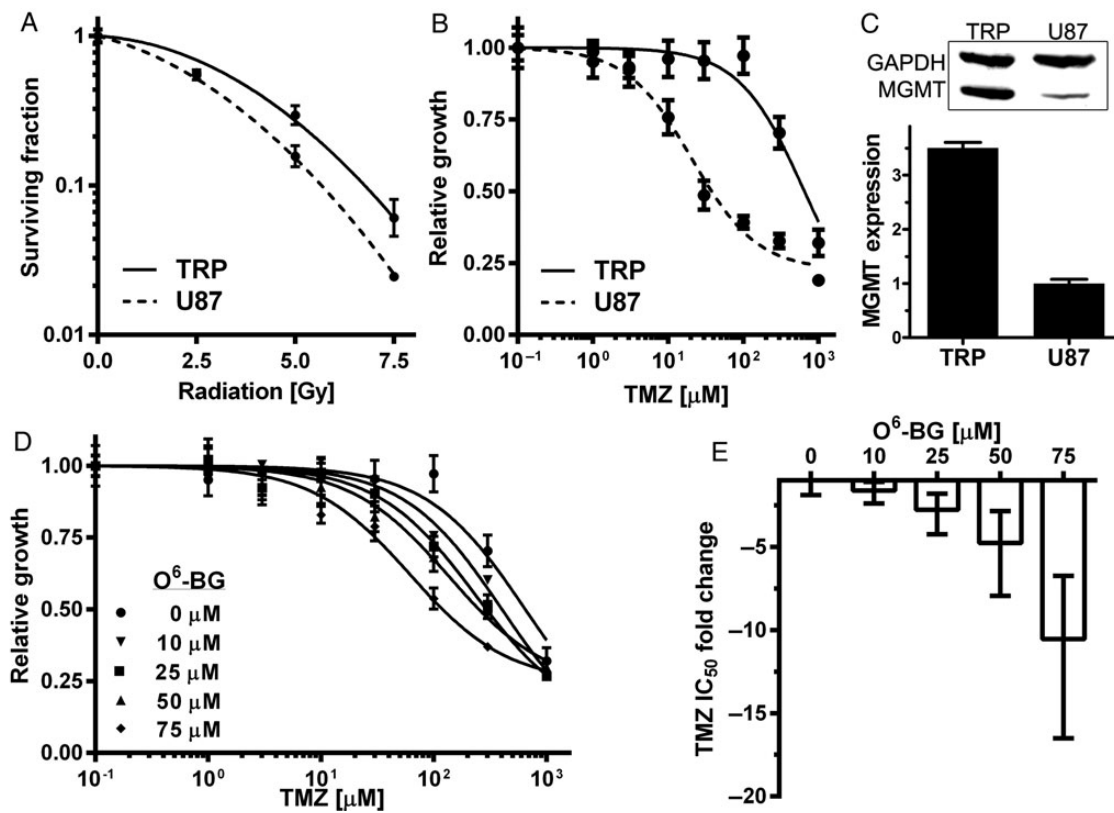


Fig. 5. TRP astrocytes are sensitive to XRT but resistant to TMZ due to MGMT. TRP astrocytes and U87 cells were sensitive to XRT ($P = .26$) (A). U87 cells (IC_{50} 21 μ M, 95% CI: 13–33 μ M) but not TRP astrocytes (IC_{50} 647 μ M, 95% CI: 409–1024 μ M) were sensitive to TMZ ($P < .0001$) (B). MGMT levels were 3.5-fold higher in TRP astrocytes ($P < .0001$) (C). The MGMT inhibitor O⁶-BG produced a dose-dependent increase in TMZ sensitivity in TRP astrocytes ($P < .0001$) (D). TMZ IC_{50} fold change from D is shown in E.

schedule were designed to achieve similar drug exposure in patients receiving 5 daily doses at 200 mg/m².² Like cultured TRP astrocytes, TRP allografts expressed MGMT (Supplementary material, Fig. S9A). XRT, but not TMZ, significantly prolonged survival (Fig. 6A). The combination decreased malignant progression (Supplementary material, Fig. S9B), but the addition of TMZ did not produce a survival benefit compared with XRT alone (Fig. 6A). Regardless of treatment, all mice eventually developed fatal astrocytomas, and the vast majority were GBMs (Supplementary material, Fig. S9B). MRI-detectable tumors developed by day 7 in control (untreated) mice, but similarly sized tumors appeared 10 days later in XRT-treated mice (Fig. 6B). XRT thus induced a transient arrest in tumor growth, but all mice succumbed from recurrent tumor.

To examine whether XRT efficacy was dependent on schedule, mice were treated with a similar total dose (16 Gy) delivered in smaller, 2 Gy daily fractions. This regimen was not as effective as 15 Gy delivered in three 5 Gy fractions, but it also significantly prolonged survival of TRP allograft mice (Supplementary material, Fig. S10A) and decreased progression to GBM (Supplementary material, Fig. S10B). We next examined whether XRT was effective in TRP allografts that had progressed to GBM (Supplementary material, Fig. S3C) by delaying treatment to day 17. XRT significantly prolonged

survival of these mice as well (Supplementary material, Fig. S10C and D).

XRT also slowed growth of luciferase-expressing TRP-Luc allografts (Fig. 6C) and significantly increased survival (Supplementary material, Fig. S11A). In contrast, XRT delayed growth but did not prolong survival of immunodeficient mice bearing orthotopic, luciferase-expressing U87FL xenografts (Supplementary material, Fig. S11B and C). Taken together, these results demonstrated that allografts derived from de-differentiated TRP astrocyte GSCs are sensitive to XRT but resistant to TMZ, due in part to their expression of MGMT.

Radiation Therapy Induces a Proneural-to-mesenchymal Shift in Transcriptome Subtype

We have shown that activating MAPK and PI3K mutations induces a primitive, proneural GBM-like gene expression state in cultured TRP astrocytes.^{13,17} Single-sample gene set enrichment analysis showed that the transcriptomes of untreated TRP allografts were also enriched for proneural signatures defined by The Cancer Genome Atlas (TCGA, Fig. 6D and Supplementary material, Fig. S11D) and Phillips et al (data not shown) in human GBM and high-grade astrocytomas, respectively.^{12,13} Transcriptome profiling of matched pairs of newly

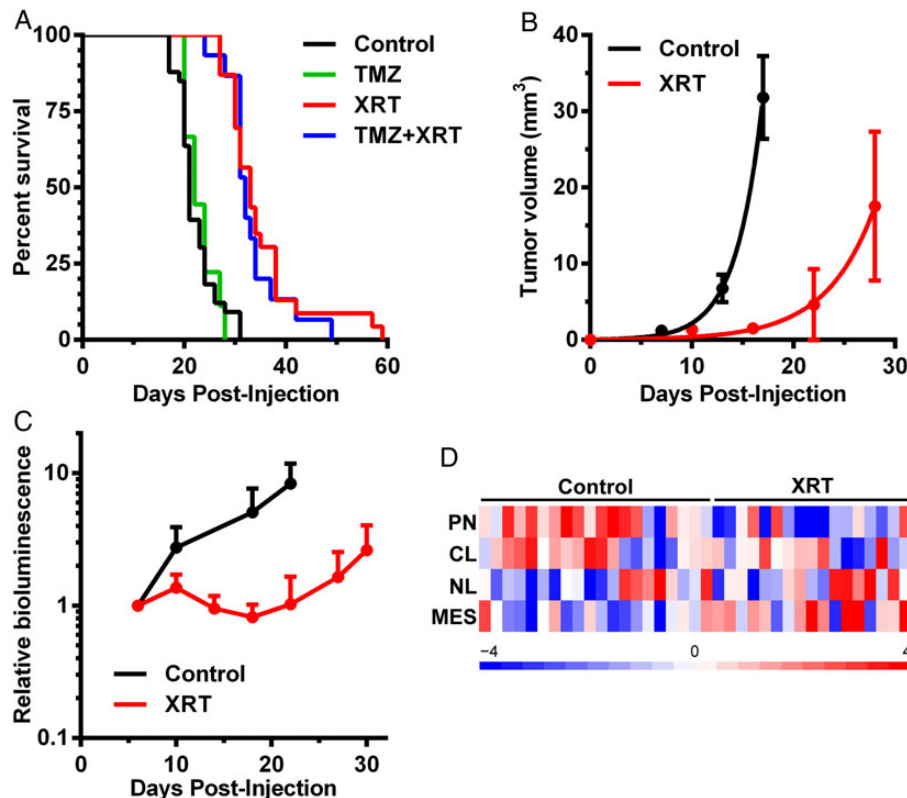


Fig. 6. Radiation therapy (XRT), but not temozolomide (TMZ), is effective in TRP allografts and induces a proneural-to-mesenchymal transcriptome shift. XRT (33 days, $P < .0001$), but not TMZ (22 days, $P = .8$), significantly prolonged median survival of TRP allograft mice (21 d). Adding TMZ did not extend survival (32 d) relative to XRT alone ($P = .5$) (A). XRT produced a significant decrease in TRP allograft growth rate by longitudinal MRI (doubling time 3.3 vs 1.8 d, $P = .002$) (B). XRT induced a similar decrease in TRP-Luc allograft growth by longitudinal BLI (doubling time 35 vs 7.7 d, $P < .0001$) (C). Transcriptomes of control, untreated TRP allografts were most similar to human proneural (PN) glioblastoma (GBM) ($P = .0005$). XRT induced a shift to mesenchymal (MES) GBM ($P = .01$) rather than classical (CL) or neural (NL) subtypes ($P \geq .2$).

diagnosed and recurrent high-grade astrocytomas from individual patients has shown that proneural tumors undergo a shift to the mesenchymal phenotype after therapy.¹² We therefore examined whether XRT induced a similar shift in TRP allograft transcriptomes. Indeed, the majority of recurrent TRP allografts were enriched for TCGA (Fig. 6D and Supplementary material, Fig. S11D) and Phillips (data not shown) mesenchymal GBM signatures. Moreover, a mesenchymal shift was also evident in the tumor microenvironment including histological evidence of mesenchymal (spindle cell) differentiation and increased expression of the mesenchymal GBM marker, vimentin (Supplementary material, Fig. S12). We therefore concluded that the TRP astrocyte-derived nGEM model mimics human proneural GBM on the histopathological, molecular, and treatment response levels.

Discussion

We have shown that G1/S ablation by T₁₂₁ alone is sufficient to induce de-differentiation of astrocytes into NSC-like cells in vitro. However, mutations that activate both MAPK and PI3K signaling were required to fully convert G1/S-defective astrocytes into GSCs capable of forming serially transplantable GBM in vivo. Similar results have been described with *Ink/arf*^{-/-} murine astrocytes that lack both gene products encoded by *Cdkn2a*: the G1/S pathway protein p16^{Ink4a} and the Trp53 pathway protein p19^{Arf}.⁴¹ In contrast to astrocytes deficient for p16^{Ink4a}, p19^{Arf}, or Trp53 alone, deletion of both *Cdkn2a* genes was required to induce de-differentiation in vitro. However, *Ink/arf*^{-/-} astrocytes were nontumorigenic. Rather, a constitutively active RTK mutation, the EGFRvIII truncation frequently found in human GBM, was required to induce high-grade gliomas in vivo. Similar results have also been described for Trp53-deficient astrocytes with activating MAPK mutations including *Nf1* deletion or *Hras*^{V12}.⁴² In contrast to astrocytes deficient for Trp53 or expressing activated *Hras*^{V12} alone, both Trp53 deletion and activating MAPK mutations were required to induce astrocyte de-differentiation in vitro and induce high-grade gliomas in vivo. Taken together, these results suggested that de-differentiation may be induced by multiple G1/S, RTK (MAPK and PI3K), and TP53 pathway mutations in gliomas of astrocyte origin.

We have extended these previous reports by showing that core GBM pathway mutations induce significant alterations in the astrocyte chromatin landscape and transcriptome. TRP astrocytes contained regions of accessible chromatin associated with genes shown to promote tumorigenesis, such as *Vav3* and *Hdac9*, as well as regions of inaccessible chromatin associated with genes that inhibit GBM tumorigenesis such as *Snai1*. Accessible chromatin regions also harbored binding motifs enriched for multiple families of stem cell-associated transcription factors including Sox and Nanog.^{43,44} RNA-seq analysis showed that TRP astrocytes mutations harbored inaccessible chromatin and downregulated expression of astrocyte signature genes including *Aqp4*, *Aldh111*, and *Fgfr3*. In contrast, stem-cell-related genes harbored accessible chromatin and increased expression including *Hoxa* locus genes (*Hoxa1*, *Hoxa5*), *Sox1*, *Sox5*, *Sox9*, and *Nfia*. These stem cell transcription factors are important for embryonic development, and their

dysregulated expression has been found in various cancers including GBM.^{32,33,45,46} These data suggest that transcription factors promoting stemness in transformed astrocytes may themselves be differentially regulated or have differential activity because of large-scale changes in their accessible chromatin landscape. Changes at the chromatin level may thus force transcription factors to alter their localization, likely driving the previously characterized gene expression differences in TRP versus T and TR astrocytes.¹⁷

The G1/S checkpoint genes *CDKN2A* and *RB1* were mutated in 61% and 9% of 281 human GBM analyzed by TCGA, respectively. Mutations in these genes were mutually exclusive (log odds ratio -1.9, $P < .0001$). Virtually all *CDKN2A* mutations were homozygous deletions affecting both *Ink4a* and *Arf* gene products. *TP53* mutations were found in 22% of these tumors and were mutually exclusive with *CDKN2A* (log odds ratio -1.4, $P < .0001$), but co-occurred with *RB1* mutations (log odds ratio -1.8, $P < .0001$).^{14,47} These findings suggest that simultaneous ablation of the G1/S checkpoint and TP53 pathways, either by *CDKN2A* deletions alone or mutations in both *RB1* and *TP53*, may function similarly to induce de-differentiation in astrocyte-derived human GBM.

The RB family of pocket proteins controls G1/S cell cycle progression and includes pRB, p107, and p130 encoded by *RB*, *RBL1*, and *RBL2*. In contrast to *RB1*, *RBL1* (0.4%) and *RBL2* (0%) mutations are extremely rare or completely absent in human GBM.^{14,47} We ablated the G1/S checkpoint in TRP astrocytes with T₁₂₁, a truncated SV40 large T antigen that functionally inactivates all 3 Rb proteins but does not affect Trp53.^{17,18,20,21} We and others have found that *Rb1* deletion alone fails to recapitulate the effects of T₁₂₁ in mouse astrocytes (Vitucci, et al, unpublished manuscript), suggesting that *Rbl1* and/or *Rbl2* compensate for *Rb1* loss in these cells.⁴⁸ Similar compensation has been found in the developing mouse eye, where *Rb1*-deficient retinoblasts fail to develop into retinoblastoma, a tumor initiated by homozygous *RB1* loss in humans. Rather, mouse retinoblasts express all 3 pocket proteins, and simultaneous deletion of *Rb1* and either *Rbl1* or *Rbl2* is required to transform these cells.⁴⁹ Furthermore, deletion of all 3 Rb genes is required to ablate the G1/S checkpoint and induce proliferation of mouse embryonic stem cells and fibroblasts.⁵⁰ Taken together, these findings suggest that humans and mice may have species-specific differences in RB family gene expression that alter their susceptibility to *RB1*-mediated tumorigenesis in particular cell types.

Transcriptome subtypes of GBM mimic the profiles of purified mouse brain cells including NSCs, astrocytes, and OPCs.^{13,14} GEM modeling studies have shown that all 3 represent candidate cells of origin for GBM.^{15,17,18,20,42,48,51,52} NSCs have received the most attention due to their phenotypic similarity to GSCs. Indeed, many mutated GBM genes, including *Rb1*, *Kras*, and *Pten*, regulate NSC self-renewal, proliferation, and differentiation in mice.⁵³⁻⁵⁵ These findings suggest that NSCs and GSCs share biological features. However, cancer cell lineage relationships are plastic.⁵⁶ The initially mutated cell may differ from the cell type that actually drives tumor growth. Indeed, genetic lineage tracing in GEM has shown that OPCs drive tumor growth when *Trp53* and *Nf1* are deleted in embryonic NSCs, suggesting that transformation is triggered only after differentiation.⁵⁷ Conversely, these mutations transform astrocytes

and induce their de-differentiation into more primitive cells.⁴² Cancer cell lineage plasticity thus precludes identifying tumor origins simply by comparing tumor transcriptomes to normal brain cells: it fails to account for mutation-induced plasticity. More extensive use of genetic lineage tracing in GBM mouse models driven by different oncogenic mutations in different cells of origin will aid in defining the cellular and genetic conditions under which lineage plasticity occurs and the extent to which it affects genomic tumor profiles.

We have previously shown that TRP mutations induce GBM in GFAP⁺ astrocytes of adult mice.²⁰ We recently used genetic lineage tracing and fate mapping to show that transformed TRP astrocytes express NSC markers within days of tumor induction, suggesting that de-differentiation occurs in situ.⁵⁸ Similar results were obtained in GEM models with alternative combinations of G1/S, MAPK-PI3K, and TP53 pathway mutations. Combining *Trp53* loss and activating MAPK mutations, including oncogenic *Hras* or *Nf1* loss, transformed mouse astrocytes, but both were required to induce de-differentiation in vitro.⁴² *Trp53* and *Pten* loss also transformed mouse astrocytes, but their effects on de-differentiation were not examined.⁴⁸ Together these results suggest that ablation of all Rb family members via *T₁₂₁* or *Cdkn2a* deletions affecting both p16^{Ink4a} and p19^{Arf}, but not *Trp53* loss alone, is sufficient to induce astrocyte de-differentiation. They also suggest that either RTK mutations (EGFRvIII) or the cooperative effects of MAPK (oncogenic Ras, *Nf1* deletion) and PI3K pathway mutations (*Pten* deletion) are required to drive de-differentiated astrocyte tumorigenesis.^{17,20,41,42,48} We conclude that cortical astrocytes, the most abundant cell type in the mammalian brain, are likely cells of origin for GBM.

GSCs are thought to be inherently resistant to XRT and chemotherapy.^{6,7} We found that de-differentiated TRP astrocyte GSCs were resistant to TMZ and expressed MGMT, like their normal NSC and astrocyte counterparts, suggesting that MGMT is one mechanism of TMZ resistance in this model system. However, an MGMT-independent mechanism is also likely, particularly the Hox/stem cell signatures that may mediate resistance in pediatric and adult GBM.^{59,60} These reports found that transcriptional activation of the *Hoxa* locus induced increased proliferation and decreased apoptosis in cultured GBM cells. These effects were abrogated by PI3K-targeted inhibitors (PI3Ki) through alterations in histone H3K27me3, and their combination with TMZ was synergistic. Together with our previous findings that a PI3K-specific signature was upregulated in TRP astrocytes and enriched in human proneural GBM,¹⁷ these results suggest that the process of TRP-induced astrocyte de-differentiation into GSCs also contributes to their TMZ resistance.

TRP allografts were enriched for proneural GBM signatures and were sensitive to XRT. Recurrent tumors were molecularly similar to XRT-treated human GBM, and XRT induced a mesenchymal shift in tumor transcriptome and morphology.¹² Similar results have been found in humans as well as a PDGF-driven mouse model of proneural GBM.^{12,61} We have therefore shown that this nGEM model system recapitulates proneural GBM on the histopathological, molecular, and treatment response levels and demonstrated its utility for preclinical experimental therapeutics. Because it employs prospectively defined oncogenic mutations in a specific cell type, this model may complement other systems used in preclinical drug development

where these factors are ambiguous, including established cell lines or patient-derived xenografts.¹⁶ It may be particularly useful for dissecting the genetics of astrocyte de-differentiation and elucidating cellular and genetic mechanisms of treatment resistance. Transplantation into syngeneic, immunocompetent hosts offers a platform for developing immunotherapies or drugs that target tumor-stroma interactions.

Funding

C.R.M. was a Damon Runyon-Genentech Clinical Investigator supported by the Damon Runyon Cancer Research Foundation (CI-45-09). R.S.M. is a Robert H. Wagner Scholar in the Molecular and Cellular Pathology Graduate Program and the Howard Hughes Medical Institute-supported Graduate Training Program in Translational Medicine. This work was supported by grants to C.R.M. from the University Cancer Research Fund (UCRF) and the Department of Defense (W81XWH-09-2-0042). The Translational Pathology Laboratory is supported by the National Institutes of Health (P30CA016086 and P30ES010126) and UCRF. The Small Animal Imaging (P30CA016086) and Confocal and Multiphoton Imaging and Bioinformatics (P30NS045892) core facilities are supported by the National Institutes of Health.

Supplementary Material

Supplementary material is available at *Neuro-Oncology Journal* online (<http://neuro-oncology.oxfordjournals.org/>).

Acknowledgments

We thank Mervi Eeva, Brian Golitz, Debbie Little, Daniel Roth, Noah Sciaky, Anna Sirbu, and Hong Yuan for technical assistance; Pablo Tamayo (Broad Institute) for single-sample gene set enrichment analysis R scripts; C. David James (UCSF) for U87FL cells; and Gary Johnson (UNC) for sequencing assistance. This work was presented in part at the 2010–2012 meetings of the American Association for Cancer Research, American Association of Neuropathologists, and Society for Neuro-oncology.

Conflict of interest statement. The authors declare no conflicts of interest.

References

- Ostrom QT, Gittleman H, Liao P, et al. CBTRUS statistical report: primary brain and central nervous system tumors diagnosed in the United States in 2007–2011. *Neuro Oncol.* 2014;16: (suppl 4):iv1–i63.
- Stupp R, Mason WP, van den Bent MJ, et al. Radiotherapy plus concomitant and adjuvant temozolomide for glioblastoma. *N Engl J Med.* 2005;352(10):987–996.
- Galli R, Binda E, Orfanelli U, et al. Isolation and characterization of tumorigenic, stem-like neural precursors from human glioblastoma. *Cancer Res.* 2004;64(19):7011–7021.
- Singh SK, Hawkins C, Clarke ID, et al. Identification of human brain tumour initiating cells. *Nature.* 2004;432(7015):396–401.
- Vescovi AL, Galli R, Reynolds BA. Brain tumour stem cells. *Nat Rev Cancer.* 2006;6(6):425–436.

6. Bao S, Wu Q, McLendon RE, et al. Glioma stem cells promote radioresistance by preferential activation of the DNA damage response. *Nature*. 2006;444(7120):756–760.
7. Beier D, Schulz JB, Beier CP. Chemoresistance of glioblastoma cancer stem cells—much more complex than expected. *Mol Cancer*. 2011;10:128.
8. Weller M, Stupp R, Reifenberger G, et al. MGMT promoter methylation in malignant gliomas: ready for personalized medicine? *Nat Rev Neurol*. 2010;6(1):39–51.
9. Hegi ME, Diserens AC, Gorlia T, et al. MGMT gene silencing and benefit from temozolomide in glioblastoma. *N Engl J Med*. 2005;352(10):997–1003.
10. Vitucci M, Hayes DN, Miller CR. Gene expression profiling of gliomas: merging genomic and histopathological classification for personalised therapy. *Br J Cancer*. 2011;104(4):545–553.
11. The Cancer Genome Atlas Research Network. Comprehensive genomic characterization defines human glioblastoma genes and core pathways. *Nature*. 2008;455(7216):1061–1068.
12. Phillips HS, Kharbanda S, Chen R, et al. Molecular subclasses of high-grade glioma predict prognosis, delineate a pattern of disease progression, and resemble stages in neurogenesis. *Cancer Cell*. 2006;9(3):157–173.
13. Verhaak RG, Hoadley KA, Purdom E, et al. Integrated genomic analysis identifies clinically relevant subtypes of glioblastoma characterized by abnormalities in PDGFRA, IDH1, EGFR, and NF1. *Cancer Cell*. 2010;17(1):98–110.
14. Brennan CW, Verhaak RG, McKenna A, et al. The somatic genomic landscape of glioblastoma. *Cell*. 2013;155(2):462–477.
15. Schmid RS, Vitucci M, Miller CR. Genetically engineered mouse models of diffuse gliomas. *Brain Res Bull*. 2012;88(1):72–79.
16. McNeill RS, Vitucci M, Wu J, Miller CR. Contemporary murine models in preclinical astrocytoma drug development. *Neuro Oncol*. 2015;17(1):12–28.
17. Vitucci M, Karpnich NO, Bash RE, et al. Cooperativity between MAPK and PI3 K signaling activation is required for glioblastoma pathogenesis. *Neuro Oncol*. 2013;15(10):1317–1329.
18. McNeill RS, Schmid RS, Bash RE, et al. Modeling astrocytoma pathogenesis in vitro and in vivo using cortical astrocytes or neural stem cells from conditional, genetically engineered mice. *J Vis Exp*. 2014;(90):e51763.
19. Prabhu A, Sarcar B, Miller CR, et al. Ras-mediated modulation of pyruvate dehydrogenase activity regulates mitochondrial reserve capacity and contributes to glioblastoma tumorigenesis. *Neuro Oncol*. 2015;17(9):1220–1230.
20. Song Y, Zhang Q, Kutlu B, et al. Evolutionary etiology of high-grade astrocytomas. *Proc Natl Acad Sci USA*. 2013;110(44):17933–17938.
21. Xiao A, Wu H, Pandolfi PP, Louis DN, Van Dyke T. Astrocyte inactivation of the pRb pathway predisposes mice to malignant astrocytoma development that is accelerated by PTEN mutation. *Cancer Cell*. 2002;1(2):157–168.
22. Dinca EB, Sarkaria JN, Schroeder MA, et al. Bioluminescence monitoring of intracranial glioblastoma xenograft: response to primary and salvage temozolomide therapy. *J Neurosurg*. 2007;107(3):610–616.
23. Buszczak M, Spradling AC. Searching chromatin for stem cell identity. *Cell*. 2006;125(2):233–236.
24. Song L, Zhang Z, Grasfeder LL, et al. Open chromatin defined by DNaseI and FAIRE identifies regulatory elements that shape cell-type identity. *Genome Res*. 2011;21(10):1757–1767.
25. Sallia B, Tran NL, Chan A, et al. The guanine nucleotide exchange factors trio, Ect2, and Vav3 mediate the invasive behavior of glioblastoma. *Am J Pathol*. 2008;173(6):1828–1838.
26. Yang R, Wu Y, Wang M, et al. HDAC9 promotes glioblastoma growth via TAZ-mediated EGFR pathway activation. *Oncotarget*. 2015;6(10):7644–7656.
27. Savary K, Caglayan D, Caja L, et al. Snail depletes the tumorigenic potential of glioblastoma. *Oncogene*. 2013;32(47):5409–5420.
28. Cahoy JD, Emery B, Kaushal A, et al. A transcriptome database for astrocytes, neurons, and oligodendrocytes: a new resource for understanding brain development and function. *J Neurosci*. 2008;28(1):264–278.
29. Lein ES, Hawrylycz MJ, Ao N, et al. Genome-wide atlas of gene expression in the adult mouse brain. *Nature*. 2007;445(7124):168–176.
30. Zeisel A, Munoz-Manchado AB, Codeluppi S, et al. Brain structure. Cell types in the mouse cortex and hippocampus revealed by single-cell RNA-seq. *Science*. 2015;347(6226):1138–1142.
31. Zhang Y, Chen K, Sloan SA, et al. An RNA-sequencing transcriptome and splicing database of glia, neurons, and vascular cells of the cerebral cortex. *J Neurosci*. 2014;34(36):11929–11947.
32. Abdel-Fattah R, Xiao A, Bomgardner D, et al. Differential expression of HOX genes in neoplastic and non-neoplastic human astrocytes. *J Pathol*. 2006;209(1):15–24.
33. Shah N, Sukumar S. The Hox genes and their roles in oncogenesis. *Nat Rev Cancer*. 2010;10(5):361–371.
34. Clark MJ, Homer N, O'Connor BD, et al. U87MG decoded: the genomic sequence of a cytogenetically aberrant human cancer cell line. *PLoS Genet*. 2010;6(1):e1000832.
35. Chalmers AJ, Ruff EM, Martindale C, Lovegrove N, Short SC. Cytotoxic effects of temozolomide and radiation are additive- and schedule-dependent. *Int J Radiat Oncol Biol Phys*. 2009;75(5):1511–1519.
36. Combs SE, Schulz-Ertner D, Roth W, Herold-Mende C, Debus J, Weber KJ. In vitro responsiveness of glioma cell lines to multimodality treatment with radiotherapy, temozolomide, and epidermal growth factor receptor inhibition with cetuximab. *Int J Radiat Oncol Biol Phys*. 2007;68(3):873–882.
37. Yang X, Darling JL, McMillan TJ, Peacock JH, Steel GG. Radiosensitivity, recovery and dose-rate effect in three human glioma cell lines. *Radiother Oncol*. 1990;19(1):49–56.
38. Agarwala SS, Kirkwood JM. Temozolomide, a novel alkylating agent with activity in the central nervous system, may improve the treatment of advanced metastatic melanoma. *Oncologist*. 2000;5(2):144–151.
39. Happend C, Roth P, Wick W, et al. Distinct molecular mechanisms of acquired resistance to temozolomide in glioblastoma cells. *J Neurochem*. 2012;122(2):444–455.
40. Chabot GG. Clinical pharmacokinetics of irinotecan. *Clin Pharmacokinet*. 1997;33(4):245–259.
41. Bachoo RM, Maher EA, Ligon KL, et al. Epidermal growth factor receptor and Ink4a/Arf: convergent mechanisms governing terminal differentiation and transformation along the neural stem cell to astrocyte axis. *Cancer Cell*. 2002;1(3):269–277.
42. Friedmann-Morvinski D, Bushong EA, Ke E, et al. Dedifferentiation of neurons and astrocytes by oncogenes can induce gliomas in mice. *Science*. 2012;338(6110):1080–1084.
43. Wegner M, Stolt CC. From stem cells to neurons and glia: a Soxist's view of neural development. *Trends Neurosci*. 2005;28(11):583–588.

44. Iv Santaliz-Ruiz LE, Xie X, Old M, Teknos TN, Pan Q. Emerging role of nanog in tumorigenesis and cancer stem cells. *Int J Cancer*. 2014; 135(12):2741–2748.
45. Sarkar A, Hochedlinger K. The sox family of transcription factors: versatile regulators of stem and progenitor cell fate. *Cell Stem Cell*. 2013;12(1):15–30.
46. Glasgow SM, Zhu W, Stolt CC, et al. Mutual antagonism between Sox10 and NFIA regulates diversification of glial lineages and glioma subtypes. *Nat Neurosci*. 2014;17(10):1322–1329.
47. Cerami E, Gao J, Dogrusoz U, et al. The cBio cancer genomics portal: an open platform for exploring multidimensional cancer genomics data. *Cancer Discov*. 2012;2(5):401–404.
48. Chow LM, Endersby R, Zhu X, et al. Cooperativity within and among Pten, p53, and Rb pathways induces high-grade astrocytoma in adult brain. *Cancer Cell*. 2011;19(3):305–316.
49. MacPherson D, Dyer MA. Retinoblastoma: from the two-hit hypothesis to targeted chemotherapy. *Cancer Res*. 2007;67(16): 7547–7550.
50. Dannenberg JH, van Rossum A, Schuijff L, te Riele H. Ablation of the retinoblastoma gene family deregulates G(1) control causing immortalization and increased cell turnover under growth-restricting conditions. *Genes Dev*. 2000;14(23):3051–3064.
51. Alcántara Llaguno S, Chen J, Kwon CH, et al. Malignant astrocytomas originate from neural stem/progenitor cells in a somatic tumor suppressor mouse model. *Cancer Cell*. 2009;15(1):45–56.
52. Galvao RP, Kasina A, McNeill RS, et al. Transformation of quiescent adult oligodendrocyte precursor cells into malignant glioma through a multistep reactivation process. *Proc Natl Acad Sci USA*. 2014;111(40):E4214–E4223.
53. Zheng H, Ying H, Yan H, et al. p53 and Pten control neural and glioma stem/progenitor cell renewal and differentiation. *Nature*. 2008;455(7216):1129–1133.
54. Sage J. The retinoblastoma tumor suppressor and stem cell biology. *Genes Dev*. 2012;26(13):1409–1420.
55. Bender RH, Haigis KM, Gutmann DH. Activated K-Ras, but not H-Ras or N-Ras, regulates brain neural stem cell proliferation in a Raf/Rb-dependent manner. *Stem Cells*. 2015;33(6): 1998–2010.
56. Meacham CE, Morrison SJ. Tumour heterogeneity and cancer cell plasticity. *Nature*. 2013;501(7467):328–337.
57. Liu C, Sage JC, Miller MR, et al. Mosaic analysis with double markers reveals tumor cell of origin in glioma. *Cell*. 2011; 146(2):209–221.
58. Irvin DM, McNeill RS, Bash RE, Miller CR. Intrinsic astrocyte heterogeneity influences tumor growth in glioma mouse models. *Brain Pathol*. 2016. DOI: 10.1111/bpa.12348.
59. Gaspar N, Marshall L, Perryman L, et al. MGMT-independent temozolomide resistance in pediatric glioblastoma cells associated with a PI3-kinase-mediated HOX/stem cell gene signature. *Cancer Res*. 2010;70(22):9243–9252.
60. Costa BM, Smith JS, Chen Y, et al. Reversing HOXA9 oncogene activation by PI3 K inhibition: epigenetic mechanism and prognostic significance in human glioblastoma. *Cancer Res*. 2010;70(2):453–462.
61. Halliday J, Helmy K, Pattwell SS, et al. In vivo radiation response of proneural glioma characterized by protective p53 transcriptional program and proneural-mesenchymal shift. *Proc Natl Acad Sci USA*. 2014;111(14):5248–5253.